Int. J. Solids Structures Vol. 21, No. 8, pp. 907–926, 1985
Printed in Great Britain.

0020-7683/85 $3.00 + .00
Pergamon Press Ltd.

ON THE EFFECTS OF ENVIRONMENTAL CONDITIONING ON RESIDUAL STRESSES IN COMPOSITE LAMINATES

B. D. HARPER
Department of Engineering Mechanics, The Ohio State University, Columbus, OH 43210-1181

Y. WEITSMAN
Mechanics and Materials Center, Civil Engineering Department, Texas A&M University, College Station, TX 77843

(*Received* 16 *January* 1984)

Abstract—This study presents an experimental and theoretical investigation of moisture effects in graphite/epoxy composites. The experiments involved exposure of antisymmetric, cross-ply laminates to various levels of fixed and fluctuating humidity and measurements of the resulting, time-dependent curvatures. Those data were compared with computed values based upon linear elasticity and linear, rheologically simple, viscoelasticity. Good agreement was noted between data and viscoelastic predictions during the moisture absorption stage from the initially dry condition. However, increasing disparity between theory and experiment developed during subsequent drying and humidity cycling conditions. This disparity is attributed to the growth of moisture-induced damage, indicating that drying and moisture cycling are more detrimental to the integrity of composites than moisture absorption, even though they may be associated with a smaller total moisture content.

INTRODUCTION

Laminated composite materials have a tendency to develop residual thermal stresses as the laminate is cooled from its elevated cure temperature. Consider, for example, a $(0/90)_s$ laminate. The thermal expansion coefficient in the direction of the fibers (longitudinal direction) is typically much smaller than the thermal expansion coefficient perpendicular to the fibers (transverse direction). In addition, the stiffness of the material parallel to the direction of the fibers is usually much greater than that transverse to the fibers. As the laminate is cooled from its elevated cure temperature, the individual laminae have a tendency to contract a much larger amount in the transverse direction relative to the longitudinal direction. However, such transverse contraction is constrained by the adjacent perpendicularly directed laminae. These adjacent-ply constraints produce residual thermal stresses in the laminate.

Linear elastic stress analysis predicts that these residual thermal stresses may exhaust the strength of various laminae in a composite structure even before the application of external loads. Effects which were attributed to high residual thermal stresses in composite laminates have been reported by several investigators[1, 2].

The polymer matrix material in composite laminates exhibits time-dependent behavior, especially at elevated temperatures or in the presence of moisture. Typically, this time-dependence reduces the magnitudes of the residual thermal stresses below those predicted by linear elasticity. There are situations, however, when this is not the case[3]. The use of elastic solutions as conservative estimates of the residual stress state in composite laminates is, therefore, often inappropriate.

It is common knowledge that the epoxy matrix material used in high performance graphite/epoxy composites absorbs moisture from a humid environment. This absorbed moisture produces expansional strains in the material which counteract the thermal contraction strains that result from the cool-down of the material from its cure temperature, and thus serve to relieve (or partially relieve) the residual thermal stresses that develop in these materials. In addition, moisture softens the epoxy matrix, substantially lowers its glass transition temperature, and accelerates its time-dependent behavior.

There is considerable evidence in the literature that, in some situations, moisture may cause irreversible time-dependent degradation of the properties of epoxy-matrix composites[4–20]. Permanent changes in certain mechanical properties[4–15] as well as changes in moisture sorption kinetics[9, 16–20] have been attributed to the presence of such time-dependent degradation.

In most instances, the decrease in graphite/epoxy composite properties (e.g. stiffness, tensile strength, etc.) due to hygrothermal exposure has been attributed to some combination of matrix degradation, and a reduction of the fiber-matrix interfacial bond strength[4]. It is generally accepted that graphite fibers, unlike glass fibers[11], do not degrade by exposure to moisture.

This study investigates the effects of post-cure cool-down and subsequent environmental conditioning upon residual stresses in composite laminates. The analysis incorporates linear viscoelastic, hygrothermorheologically simple material behavior with classical laminated plate theory to predict the time-dependent hygrothermal stresses as well as the mid-plane strains and curvatures of antisymmetric cross-ply graphite/epoxy laminates. For comparison, the analysis is also performed assuming that the material behavior is linearly elastic.

Experimental assessment of residual stresses was provided by measurements of the time-dependent curvature of antisymmetric cross-ply $(0/90/0_4/90_4/0/90)_T$ AS/3502 graphite/epoxy laminates. These measurements were then compared with linear elastic and viscoelastic predictions.

Even though the elastic and viscoelastic analyses do not consider irreversible moisture-induced degradation, careful attention was paid to all experimental data in order to detect the presence of such effects.

ELASTIC FORMULATION

Consider an antisymmetric cross-ply laminate, depicted in Fig. 1, exposed to fluctuating ambient temperature $T(t)$ and relative humidity $\phi(t)$. In view of the high thermal diffusivity and the small thickness of composite laminates employed in practice, it is permissible to ignore the process of thermal diffusion and employ the approximation that $T = T(t)$ throughout the laminate. On the other hand, the slowness of the process of moisture diffusion requires taking full account of transient moisture distributions. For laminates of thickness much smaller than in-plane dimensions, moisture diffusion may be considered spatially one-dimensional.

Employing the assumptions of classical laminated plate theory[21], the linear elastic stress/strain relations for the odd-numbered, orthotropic plies in Fig. 1 are

$$\begin{aligned}\sigma_x(z,t) &= C_L(\epsilon_x^0(t) + zk_x(t) - \alpha_L\Delta T(t) - \beta_L m_e(z,t)) \\ &\quad + C_{LT}(\epsilon_y^0(t) + zk_y(t) - \alpha_T\Delta T(t) - \beta_T m_e(z,t)) \\ \sigma_y(z,t) &= C_{LT}(\epsilon_x^0(t) + zk_x(t) - \alpha_L\Delta T(t) - \beta_L m_e(z,t)) \\ &\quad + C_T(\epsilon_y^0(t) + zk_y(t) - \alpha_T\Delta T(t) - \beta_T m_e(z,t)).\end{aligned} \tag{1}$$

In (1), σ denotes stress, ϵ^0 and k the mid-plane strain and curvature, respectively, C designates stiffness, and α and β are linear thermal and moisture expansion coefficients. Also, ΔT denotes temperature change and m_e the effective moisture content

$$\begin{aligned}m_e(z,t) &= m(z,t) - m_1 \quad \text{for} \quad m(z,t) > m_1 \\ &= 0 \quad \text{for} \quad m(z,t) \le m_1,\end{aligned} \tag{2}$$

where $m(z,t)$ is the moisture content and m_1 the "threshold" moisture content, below which no moisture expansional strains are observed. The subscripts L and T in eqn (1) denote properties parallel and transverse to the direction of the fibers respectively, while subscripts x and y refer to the laminate coordinate system of Fig. 1.

The stress/strain relations for the even-numbered plies are obtained by interchanging subscripts L and T in eqn (1).

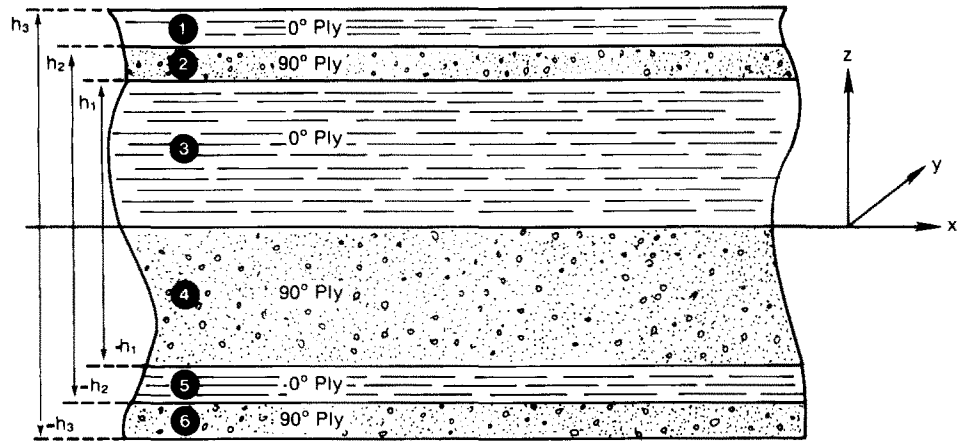

Fig. 1. Geometry of antisymmetric cross-ply laminate.

Because the laminate is assumed to be free of external loading, the net resultant forces and moments on the laminate must vanish, thus

$$\begin{aligned} N_x(t) &= \int_{-h_3}^{h_3} \sigma_x(z, t)\, dz = 0 \\ N_y(t) &= \int_{-h_3}^{h_3} \sigma_y(z, t)\, dz = 0 \\ M_x(t) &= \int_{-h_3}^{h_3} \sigma_x(z, t)\, z\, dz = 0 \\ M_y(t) &= \int_{-h_3}^{h_3} \sigma_y(z, t)\, z\, dz = 0. \end{aligned} \tag{3}$$

Appropriate substitutions into (3), followed by integration of the expressions, yields four equations in the unknowns ϵ_x^0, ϵ_y^0, k_x, and k_y. Solution of these equations yields

$$\begin{aligned} \epsilon_x^0(t) = \epsilon_y^0(t) &= \frac{1}{\Delta}\,[h_3^3(C_L + C_T - 2C_{LT})\,\{h_3(P + Q)\Delta T(t) + (R + S)F(t)\} \\ &\quad - 3g_1(C_L - C_T)\,\{g_1(P - Q)\Delta T(t) + (R - S)G(t)\}] \\ k_x(t) = -k_y(t) &= \frac{3}{\Delta}\,[h_3(C_L + C_T + 2C_{LT})\,\{g_1(P - Q)\Delta T(t) + (R - S)G(t)\} \\ &\quad - g_1(C_L - C_T)\,\{h_3(P + Q)\Delta T(t) + (R + S)F(t)\}], \end{aligned} \tag{4}$$

where

$$\begin{aligned} P &= C_L\alpha_L + C_T\alpha_T \\ Q &= C_{LT}\alpha_L + C_T\alpha_T \\ R &= C_L\beta_L + C_{LT}\beta_T \\ S &= C_{LT}\beta_T + C_T\beta_T \\ g_1 &= \frac{1}{2}h_3^2 + h_1^2 - h_2^2 \\ \Delta &= h_3^4\,\{(C_L + C_T)^2 - 4C_{LT}^2\} - 3g_1^2\,(C_L - C_T)^2 \\ F(t) &= \int_0^{h_3} m_e(z, t)\, dz \\ G(t) &= \int_0^{h_3} m_e(z, t)z\, dz - 2\int_{h_1}^{h_2} m_e(z, t)z\, dz. \end{aligned}$$

Note that the moisture content profile $m(z, t)$ is found independently by solving the diffusion equation.

Once ϵ_x^0 and k_x are determined from (4), the stresses may be obtained by direct substitution into (1).

VISCOELASTIC FORMULATION

For the viscoelastic case, the material behavior is assumed to be hygrothermorheologically simple and linear. Making the assumptions of classical laminated plate theory, and noting again that $\epsilon_x^0 = \epsilon_y^0$ and $k_x = -k_y$ due to the antisymmetric cross-ply lay-up, we have the following relations for the odd-numbered plies:

$$\begin{aligned}
\sigma_x(z, t) &= \int_0^t C_L(\xi - \xi') \left\{ \frac{\partial \epsilon_x^0(\tau)}{\partial \tau} + z \frac{\partial k_x(\tau)}{\partial \tau} - \frac{\partial(\alpha_L \Delta T(\tau))}{\partial \tau} - \beta_L \frac{\partial m_e(z, \tau)}{\partial \tau} \right\} d\tau \\
&\quad + \int_0^t C_{LT}(\xi - \xi') \left\{ \frac{\partial \epsilon_x^0(\tau)}{\partial \tau} - z \frac{\partial k_x(\tau)}{\partial \tau} - \frac{\partial(\alpha_T \Delta T(\tau))}{\partial \tau} - \beta_T \frac{\partial m_e(z, \tau)}{\partial \tau} \right\} d\tau \\
\sigma_y(z, t) &= \int_0^t C_{LT}(\xi - \xi') \left\{ \frac{\partial \epsilon_x^0(\tau)}{\partial \tau} + z \frac{\partial k_x(\tau)}{\partial \tau} - \frac{\partial(\alpha_L \Delta T(\tau))}{\partial \tau} - \beta_L \frac{\partial m_e(z, \tau)}{\partial \tau} \right\} d\tau \\
&\quad + \int_0^t C_T(\xi - \xi') \left\{ \frac{\partial \epsilon_x^0(\tau)}{\partial \tau} - z \frac{\partial k_x(\tau)}{\partial \tau} - \frac{\partial(\alpha_T \Delta T(\tau))}{\partial \tau} - \beta_T \frac{\partial m_e(z, \tau)}{\partial \tau} \right\} d\tau.
\end{aligned} \tag{6}$$

Expressions for the even-numbered plies are obtained by interchanging subscripts L and T in (6). In eqn (6), the reduced times ξ and ξ' are defined by

$$\begin{aligned}
\xi &= \xi(z, t) = \int_0^t \frac{ds}{a_{TM}(m(z, s), T(s))} \\
\xi' &= \xi'(z, \tau) = \int_0^\tau \frac{ds}{a_{TM}(m(z, s), T(s))},
\end{aligned} \tag{7}$$

where a_{TM} is the combined temperature-moisture shift factor.

Requiring net resultant forces and moments to vanish at all times results in two integral equations

$$\begin{aligned}
&\int_0^t \left(\int_0^{h_3} F_1(\xi - \xi')\, dz \right) \frac{\partial \epsilon_x^0(\tau)}{d\tau} d\tau + \int_0^t \left(\int_0^{h_3} F_3(\xi - \xi') z\, dz \right. \\
&\quad \left. - 2 \int_{h_1}^{h_2} F_3(\xi - \xi') z\, dz \right) \frac{\partial k_x(\tau)}{\partial \tau} d\tau = R_1(t) \\
&\int_0^t \left(\int_0^{h_3} F_3(\xi - \xi') z\, dz - 2 \int_0^{h_2} F_3(\xi - \xi') z\, dz \right) \frac{\partial \epsilon_x^0(\tau)}{\partial \tau} d\tau \\
&\quad + \int_0^t \left(\int_0^{h_3} F_2(\xi - \xi') z^2\, dz \right) \frac{\partial k_x(\tau)}{\partial \tau} d\tau = R_2(t),
\end{aligned} \tag{8}$$

where

$$\begin{aligned}
R_1(t) &= \int_0^t \left(\int_0^{h_3} F_4(\xi - \xi')\, dz \right) \frac{\partial[\alpha_T(T(\tau)) \Delta T(\tau)]}{d\tau} d\tau \\
&\quad + \int_0^t \left(\int_0^{h_3} F_5(\xi - \xi')\, dz \right) \frac{\partial[\alpha_L(T(\tau)) \Delta T(\tau)]}{d\tau} d\tau \\
&\quad + \int_0^t \left(\int_0^{h_3} (F_4(\xi - \xi') \beta_T + F_5(\xi - \xi') \beta_L) \frac{\partial m_e(z, \tau)}{\partial \tau} dz \right) d\tau
\end{aligned}$$

$$R_2(t) = \int_0^t \left(\int_0^{h_3} F_7(\xi - \xi')z \, dz - 2\int_{h_1}^{h_2} F_7(\xi - \xi')z \, dz \right) \frac{\partial[\alpha_T(T(\tau))\Delta T(\tau)]}{\partial\tau} d\tau \quad (9)$$

$$+ \int_0^t \left(\int_0^{h_3} F_6(\xi - \xi')z \, dz - 2\int_{h_1}^{h_2} F_6(\xi - \xi')z \, dz \right) \frac{\partial[\alpha_T(T(\tau))\Delta T(\tau)]}{\partial\tau} d\tau$$

$$+ \int_0^t \left\{ \int_0^{h_3} (F_7(\xi - \xi')\beta_T + F_6(\xi - \xi')\beta_L) \frac{\partial m_e(z, \tau)}{\partial\tau} z \, dz \right.$$

$$\left. - 2\int_{h_1}^{h_2} (F_7(\xi - \xi')\beta_T + F_6(\xi - \xi')\beta_L) \frac{\partial m_e(z, \tau)}{\partial\tau} z \, dz \right\} d\tau$$

and

$$\begin{aligned} F_1 &= C_L + C_T + 2C_{LT}; & F_5 &= C_L + C_{LT} \\ F_2 &= C_L + C_T - 2C_{LT}; & F_6 &= C_L - C_{LT} \\ F_3 &= C_L - C_T; & F_7 &= C_{LT} - C_T \\ F_4 &= C_T + C_{LT}. \end{aligned} \quad (10)$$

MOISTURE DIFFUSION

For many epoxy resin composites, the moisture sorption process was found to follow the classical diffusion equation[16]:

$$\frac{\partial m}{\partial t} = D \frac{\partial^2 m}{\partial z^2}, \quad (11)$$

where m is the moisture content, t denotes time, and z is the spatial coordinate for one-dimensional diffusion. Also, D is the moisture diffusion coefficient.

In many circumstances, the equilibrium moisture content M_∞ was correlated to the ambient relative humidity ϕ[19, 22, 23], and for the composite material at hand it was found[23]:

$$M_\infty = 0.00268\phi^{1.325}. \quad (12)$$

Finally, the coefficient D in eqn (11) was found to vary most significantly with temperature[16, 23]. For the present case we have[23]

$$D = D(T) = 1.67 \exp(-5480/T). \quad (13)$$

In eqn (13), T denotes temperature in $^\circ K$ and D is in mm^2/sec.

The solution to (11) is well known[24, 25] and can be evaluated most efficiently by a scheme proposed recently[26]. This scheme will be followed for calculating moisture profiles to be inserted in (1) and (6).

NUMERICAL PROCEDURES

The complexity of the viscoelastic integral equations (8) necessitates the use of a numerical solution. Conventional numerical integration procedures are inappropriate because the unknown functions to be determined, namely $\epsilon_x^0(t)$ and $k_x(t)$, appear as derivatives within the integral.

An approach often referred to as the "incremental time-marching scheme" has been employed on several occasions to solve integral equations of this type[23, 27, 28].

To illustrate this method, consider one of the integral expressions in (8), namely

$$I(t) = \int_0^t \left(\int_0^{h_3} F_1(\xi(z, t) - \xi(z, \tau))\, dz \right) \frac{\partial \epsilon_x^0(\tau)}{\partial \tau}\, d\tau \tag{14}$$

with

$$\xi(z, u) = \int_0^u \frac{ds}{a_{TM}(m(z, s), T(s))}. \tag{15}$$

First discretize the time domain into M time steps, not necessarily equal in magnitude. Evaluating (14) at time $t = t_j$, and allowing for the possibility of discontinuity at time $t = 0$, we have

$$\begin{aligned} I(t_j) &= \int_0^{h_3} F_1(\xi(z, t_j))\, dz\, [\epsilon_x^0(0^+) - \epsilon_x^0(0^-)] \\ &\quad + \sum_{k=0}^{j-1} \int_{t_k}^{t_{k+1}} \left(\int_0^{h_3} F_1(\xi(z, t_j) - \xi(z, \tau))\, dz \right) \frac{\partial \epsilon_x^0(\tau)}{\partial \tau}\, d\tau \\ &\simeq \int_0^{h_3} F_1(\xi(z, t_j))\, dz\, [\epsilon_x^0(0^+) - \epsilon_x^0(0^-)] \\ &\quad + \frac{1}{2} \sum_{k=0}^{j-1} \left\{ \int_0^{h_3} [F_1(\xi(z, t_j) - \xi(z, t_{k+1})) \right. \\ &\quad \left. + F_1(\xi(z, t_j) - \xi(z, t_k))]\, dz \right\} [\epsilon_x^0(t_{k+1}) - \epsilon_x^0(t_k)] \end{aligned} \tag{16}$$

where $t_0 \equiv 0^+$.

The spatial integration in eqn (16) is performed by discretizing the laminate half-thickness, h_3, into N divisions, again not necessarily equal in magnitude, for example

$$\begin{aligned} \int_0^{h_3} F_1(\xi(z, t_j) - \xi(z, t_k))\, dz &\simeq \frac{1}{2} \sum_{i=0}^{N-1} \{F_1(\xi(z_{i+1}, t_j) - \xi(z_{i+1}, t_k)) \\ &\quad + F_1(\xi(z_i, t_j) - \xi(z_i, t_k))\} (z_{i+1} - z_i) \end{aligned} \tag{17}$$

where $z_0 \equiv 0$ and $z_N \equiv h_3$.

Upon discretization of all terms in (8), it is finally possible to form two equations in the unknown quantities $\epsilon_x^0(t_j)$ and $k_x(t_j)$ that can be solved simultaneously. Note that at time $t = t_j$, all earlier values $\epsilon_x^0(t_1), \ldots, \epsilon_x^0(t_{j-1})$ and $k_x(t_1), \ldots, k_x(t_{j-1})$ are known from previous steps. With $\epsilon_x^0(t_j)$ and $k_x(t_j)$ known, one then increments the time to $t = t_{j+1}$ and proceeds as above to find $\epsilon_x^0(t_{j+1})$ and $k_x(t_{j+1})$. This procedure is repeated progressively until the mid-plane strain and curvature are found at any time of interest.

Note that this procedure requires solving for ϵ_x^0 and k_x at each time increment, even though these values may only be desired at the final time $t = t_M$ or perhaps at only a few of the intermediate times. For this reason, this procedure is rather inefficient for very long hygrothermal histories.

In order to improve numerical efficiency, a method similar to that proposed by Schapery[29] was employed to solve eqn (8) for the time-dependent mid-plane strains and curvatures. This method involves approximating the mid-plane strains and curvatures by the functions $\epsilon_x^{(1)}$ and $k_x^{(1)}$ defined through the following expressions:

$$\begin{aligned} \left(\int_0^{h_3} F_1(\xi)\, dz \right) \epsilon_x^{(1)} + \left(\int_0^{h_3} F_3(\xi) z\, dz - 2 \int_{h_1}^{h_2} F_3(\xi) z\, dz \right) k_x^{(1)} &= R_1(t) \\ \left(\int_0^{h_3} F_3(\xi) z\, dz - 2 \int_{h_1}^{h_2} F_3(\xi) z\, dz \right) \epsilon_x^{(1)} + \left(\int_0^{h_3} F_2(\xi) z^2\, dz \right) k_x^{(1)} &= R_2(t), \end{aligned} \tag{18}$$

where $R_1(t)$ and $R_2(t)$ are given in (9) and $\xi = \xi(z, t)$ is given in (7). Note that $R_1(t)$ and $R_2(t)$ can be evaluated exactly at any time of interest since the temperature and moisture history is known explicitly beforehand. Therefore, the approximate quantities $\epsilon_x^{(1)}$ and $k_x^{(1)}$ do not need to be known at each intermediate time step in the numerical integration process, as was required in the previous procedure.

In order to estimate the error involved in using $\epsilon_x^{(1)}$ and $k_x^{(1)}$ as the mid-plane strain and curvature, define

$$\begin{aligned} \Delta\epsilon_x &= \epsilon_x^0 - \epsilon_x^{(1)} \\ \Delta k_x &= k_x - k_x^{(1)}. \end{aligned} \tag{19}$$

Manipulations of (8) and (18) then yield the following integral expressions for $\Delta\epsilon_x$ and Δk_x,

$$\begin{aligned} &\int_0^t \left(\int_0^{h_3} F_1(\xi - \xi')\, dz \right) \frac{\partial \Delta\epsilon_x}{\partial\tau}\, d\tau + \int_0^t \left(\int_0^{h_3} F_3(\xi - \xi')z\, dz \right. \\ &\left. - 2\int_{h_1}^{h_2} F_3(\xi - \xi')z\, dz \right) \frac{\partial \Delta k_x}{\partial\tau}\, d\tau = \int_0^t \left\{ \int_0^{h_3} (F_1(\xi) - F_1(\xi - \xi'))\, dz \right\} \frac{\partial \epsilon_x^{(1)}}{\partial\tau}\, d\tau \\ &+ \int_0^t \left\{ \int_0^{h_3} (F_3(\xi) - F_3(\xi - \xi'))z\, dz - 2\int_{h_1}^{h_2} (F_3(\xi) - F_3(\xi - \xi'))z\, dz \right\} \frac{\partial k_x^{(1)}}{\partial\tau}\, d\tau \end{aligned} \tag{20}$$

$$\begin{aligned} &\int_0^t \left(\int_0^{h_3} F_3(\xi - \xi')z\, dz - 2\int_{h_1}^{h_2} F_3(\xi - \xi')z\, dz \right) \frac{\partial \Delta\epsilon_x}{\partial\tau}\, d\tau \\ &+ \int_0^t \left(\int_0^{h_3} F_2(\xi - \xi')z^2\, dz \right) \frac{\partial \Delta k_x}{\partial\tau}\, d\tau = \int_0^t \left\{ \int_0^{h_3} (F_3(\xi) - F_3(\xi - \xi'))z\, dz \right. \\ &\left. - 2\int_{h_1}^{h_2} (F_3(\xi) - F_3(\xi - \xi'))z\, dz \right\} \frac{\partial \epsilon_x^{(1)}}{\partial\tau}\, d\tau + \int_0^t \left\{ \int_0^{h_3} (F_2(\xi) \right. \\ &\left. - F_2(\xi - \xi'))z^2\, dz \right\} \frac{\partial k_x^{(1)}}{\partial\tau}\, d\tau. \end{aligned} \tag{21}$$

The solution of (20) and (21) for $\Delta\epsilon_x$ and Δk_x will involve the same incremental time-marching procedure as mentioned previously, but since the "errors" $\Delta\epsilon_x$ and Δk_x are presumably small in comparison with $\epsilon_x^{(1)}$ and $k_x^{(1)}$, it is possible to employ cruder time-steps in the numerical integration.

If $\Delta\epsilon_x \ll \epsilon_x^{(1)}$ and $\Delta k_x \ll k_x^{(1)}$ then $\epsilon_x^{(1)} + \Delta\epsilon_x$ and $k_x^{(1)} + \Delta k_x$ may be taken as our solution. Otherwise, higher-order increments $\Delta^{(2)}\epsilon_x$ and $\Delta^{(2)}k_x$ can be calculated in a similar manner.

In our case, $\Delta\epsilon_x$ and Δk_x provided sufficient accuracy, because they resulted in corrections of no more than a few percentage points.

SUMMARY OF MATERIAL PROPERTIES

Published data on the AS/3502 graphite/epoxy material[30] indicate that only the transverse compliance S_T shows any appreciable time-dependence. The compliances S_L and S_{LT} were both virtually constant with values given by

$$\begin{aligned} S_L &= 8.00 \times 10^{-6}\ \text{MPa}^{-1} \\ S_{LT} &= 2.32 \times 10^{-6}\ \text{MPa}^{-1}. \end{aligned} \tag{22}$$

The dry transverse compliance data can be expressed in the following form:

$$S_T(t) = S_0(t + t_0)^q \tag{23}$$

with

$$\begin{aligned} S_0 &= 88.2 \times 10^{-6}\ \text{MPa}^{-1}\cdot\text{min}^{-q} \\ q &= 0.00775 \\ t_0 &= 1\ \text{min}, \end{aligned} \tag{24}$$

while wet transverse compliance data assumed the form

$$S_T(t) = D_0 + D_1 t^n \tag{25}$$

with

$$\begin{aligned} D_0 &= 88.2 \times 10^{-6}\ \text{MPa}^{-1} \\ D_1 &= 1.662 \times 10^{-6}\ \text{MPa}^{-1}\ \text{min}^{-n} \\ n &= 0.14. \end{aligned} \tag{26}$$

The data also indicate that the AS/3502 material is hygrothermorheologically simple. The temperature-dependent shift factor, a_T, and moisture dependent shift factor, a_M, were expressed as follows

$$a_T = \exp(-T/A + B) \tag{27}$$

and

$$a_M = \exp(-C_0 m + C_1) \tag{28}$$

with

$$\begin{aligned} A &= 6.258 \\ B &= 45.81 \\ C_0 &= 5.2 \\ C_1 &= .26. \end{aligned} \tag{29}$$

In (27) and (28), T is the temperature in °K and m is the moisture content in % weight gain.

It was also found that the combined temperature-moisture shift factor, a_{TM}, could be expressed as a product

$$a_{TM} = a_T a_M. \tag{30}$$

Data from reference [30] also indicate that the thermal expansion coefficient varies linearly with temperature

$$\begin{aligned} \alpha_L &= \alpha_{L0} + \alpha_{L1} T \\ \alpha_T &= \alpha_{T0} + \alpha_{T1} T \end{aligned} \tag{31}$$

with

$$\begin{aligned} \alpha_{L0} &= -.484 \times 10^{-6}\ \text{cm/cm/°K} \\ \alpha_{L1} &= 0.72 \times 10^{-9}\ \text{cm/cm/°K}^2 \\ \alpha_{T0} &= 9.05 \times 10^{-6}\ \text{cm/cm/°K} \\ \alpha_{T1} &= 0.41 \times 10^{-7}\ \text{cm/cm/°K}^2. \end{aligned} \tag{32}$$

Experimental data on AS/3502 graphite/epoxy[23] indicate that transverse moisture expansional strains may be expressed

$$\begin{aligned} \epsilon_T^H &= \beta_T(m - m_1) \quad \text{for} \quad m > m_1 \\ \epsilon_T^H &= 0 \quad \text{for} \quad m \leq m_1, \end{aligned} \tag{33}$$

where ϵ_T^H is the transverse moisture swelling strain, m is the moisture content, and m_1 the threshold moisture content ($m_1 = 0.1\%$). Also, β_T is the transverse moisture expansion coefficient ($\beta_T = 0.00324$ cm/cm/% moisture).

The longitudinal moisture expansional strain was negligibly small and we took $\beta_L = 0$ in all computations.

Because data for the AS/3502 material[30] are given in terms of creep compliances, we employed the quasi-elastic approximation[31] to express the relaxation moduli that are required for our viscoelastic analysis, namely

$$\begin{aligned} C_L(t) &= \frac{S_T(t)}{S_L S_T(t) - S_{LT}^2} \\ C_T(t) &= \frac{S_L}{S_L S_T(t) - S_{LT}^2} \\ C_{LT}(t) &= \frac{-S_{LT}}{S_L S_T(t) - S_{LT}^2}. \end{aligned} \tag{34}$$

It has been shown[23] that for the AS/3502 material, the above approximation involves errors of less than 2%.

EXPERIMENTAL PROCEDURE

Effects of residual stresses in composite materials can be detected by measuring curvatures of antisymmetric laminates[2, 4, 23, 28, 32–34]. However, both lay-up and dimensions of the laminate must be chosen advisedly. For instance, the easiest conceivable lay-up, that of $[0_n/90_n]_T$ is unsuitable because it develops premature cracks due to its low fracture toughness[2, 28, 33]. In addition, the deformation of plates with high length-to-thickness ratios departs from linearity, and may be even subjected to thermal buckling[35], while excessively thick plates require an impractically long time to reach moisture saturation.

Based on a multitude of considerations[23], square plates of in-plane dimensions of 0.1016 m (4″) and the lay-up $[0/90/0_4/90_4/0/90]_T$ were chosen as test specimens (see Fig. 1). Forty-five specimens were cut up from larger panels that were manufactured and cured according to manufacturer's specifications.

Curvatures were determined from deflections that were measured periodically by means of dial gages attached to a rigid stand, as detailed elsewhere[23]. Deflection measurements yielded no more than 1% deviations in curvature values within each specimen and a scatter of $\pm 4\%$ within each group of specimens. Also, the curvatures k_x and k_y deviated from their average values by no more than 4%.

Exposure to fixed levels of relative humidity was achieved by placing specimens above suitable salt solutions[36] within humidity chambers.* Temperature control was achieved by placing the chambers in several rooms with different thermostat settings. A summary of the test environments is given in Table 1 below.

To assure initially dry conditions, all specimens were dessicated at 327°K (130°F) until reaching equilibrium weight. Upon exposure to moisture, weight gains were measured periodically, at equal $t^{1/2}$ intervals.

* The selected solutions were: LiCl (13%R.H.), NaCl (75%R.H.), and K_2SO_4 (95%R.H.).

Table 1. Combinations of temperature and relative humidity considered

T (°K) \ RH (%)	0	13	75	95
298		X	X	X
327	X	X	X	X
339	X	X	X	X
346				X

RESULTS

Computational and experimental results for all environmental exposures are shown in Figs. 2–11. In all those figures, values of the nondimensional *curvature change* $h_3(k_{x_i} - k_x(t))$ are plotted versus the square root of time, t, in days. In the above, h_3 is half the laminate thickness as before, k_{x_i} is the initial dry curvature and $k_x(t)$ is the time-dependent curvature. The solid lines in the figures refer to elastic predictions, whereas dashed lines represent viscoelastic evaluations. Experimentally determined curvatures had a typical data scatter of about 4–6%, about the average values shown in the figures.

In those cases which include desorption (Figs. 2–4), the desorption results were plotted with the time scale reset and measured as the square root of time since the initiation of desorption.

In view of the observation that a geometrically constrained Hercules 3502 resin develops significant chemical shrinkage stresses during cure[37], the initial curvature, prior to exposure to moisture, is caused partly by the above-mentioned chemical effect and partly by thermal cool-down. Because it is impossible to separate those effects, it

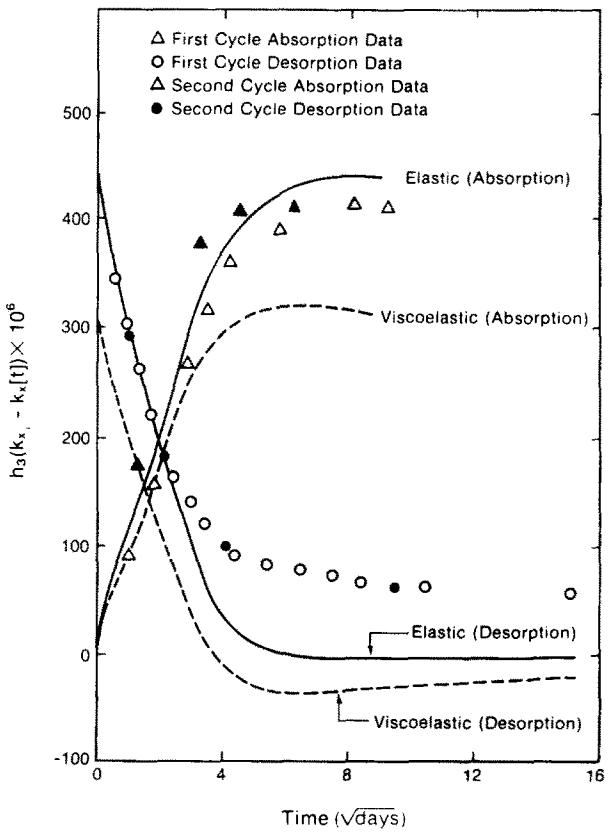

Fig. 2. Time-dependent curvature change of $(0/90/0_4/90_4/0/90)_T$ AS/3502 graphite/epoxy laminates at 346°K (163°F). Absorption data is obtained at 95% relative humidity.

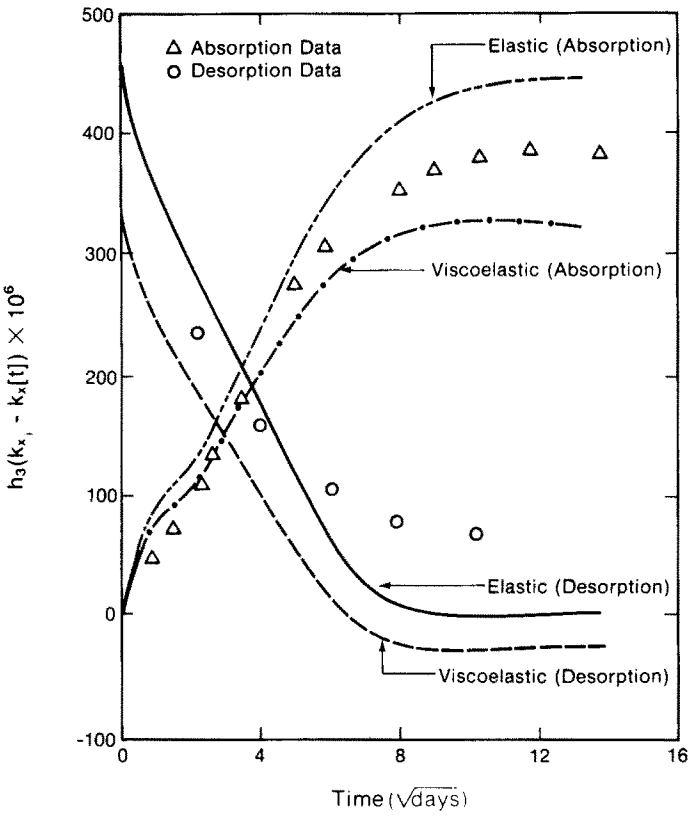

Fig. 3. Time-dependent curvature change of $(0/90/0_4/90_4/0/90)_T$ AS/3502 graphite/epoxy laminates at 339°K (150°F). Absorption data is obtained at 95% relative humidity.

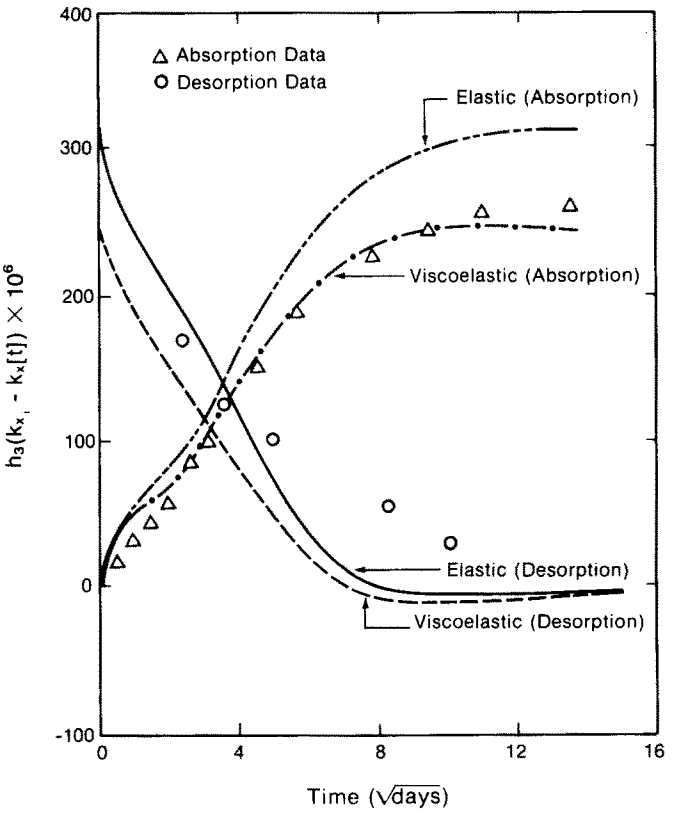

Fig. 4. Time-dependent curvature change of $(0/90/0_4/90_4/0/90)_T$ AS/3502 graphite/epoxy laminates at 339°K (150°F). Absorption data is obtained at 75% relative humidity.

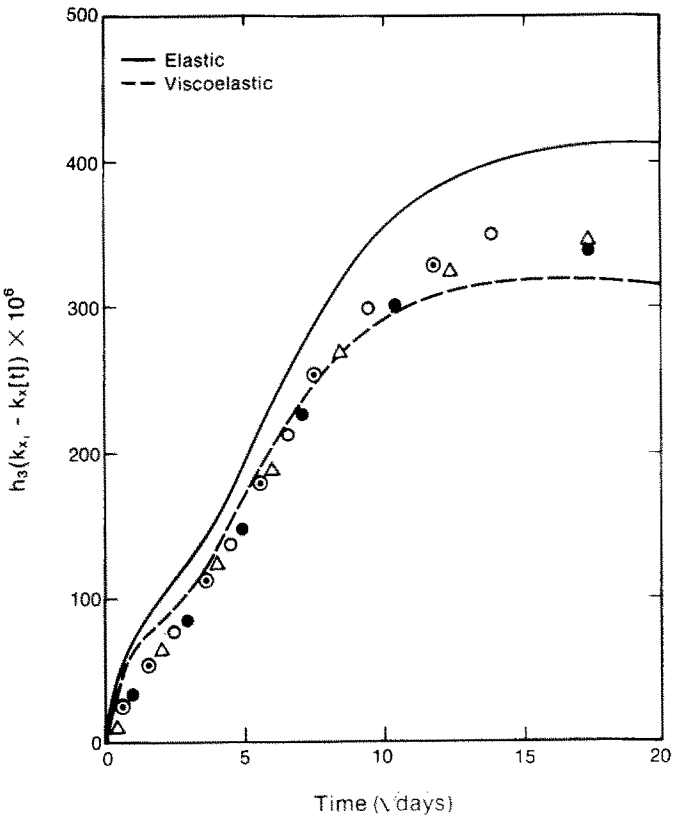

Fig. 5. Time-dependent curvature change of $(0/90/0_4/90_4/0/90)_T$ AS/3502 graphite/epoxy laminates during absorption at 327°K (130°F) 95% relative humidity.

was decided to relate all results in terms of departures from an initial curvature, rather than through absolute curvatures. Presented in this manner, the effects of initial stresses should disappear entirely in the elastic case. However, the uncertainty regarding initial stress effects must still be resolved when considering viscoelastic behavior. To overcome this ambiguity, two sets of viscoelastic computations were performed. In the first set, the stress-free temperature was assumed to be the cure temperature of 455°K (350°F), while in the second set, the stress-free temperature was assumed to be 25°K higher. It was found that the results of the two sets of calculations yielded indistinguishable results for the *curvature differences* $k_{x_i} - k_x(t)$ that are exhibited in Figs. 2–11.

Reproducibility of experimental results was checked by exposing two groups, of three specimens each, in two separate chambers to identical environmental conditions. The results for all four groups, averaging values between the three specimens within each group, are shown in Fig. 5. It is seen that the results coalesce to a continuous curve, proving consistent and reproducible data.

Note that, because of the way results are plotted in Figs. 2–11, large values of the ordinate represent greater change of the curvature relative to the initial dry curvature, and thus smaller absolute values of curvature. It is interesting to note that elasticity predicts greater departures of curvature than viscoelasticity. In addition, during desorption the viscoelastic curvature exceeds its earlier value, prior to the onset of conditioning. These results seem contrary to intuitive notions that relaxation behavior should necessarily yield values that are smaller. However, they are typical of results obtained for problems in which an external agent (in this case moisture) acts as a stress-inducing agent as well as a stress-relaxing factor[3].

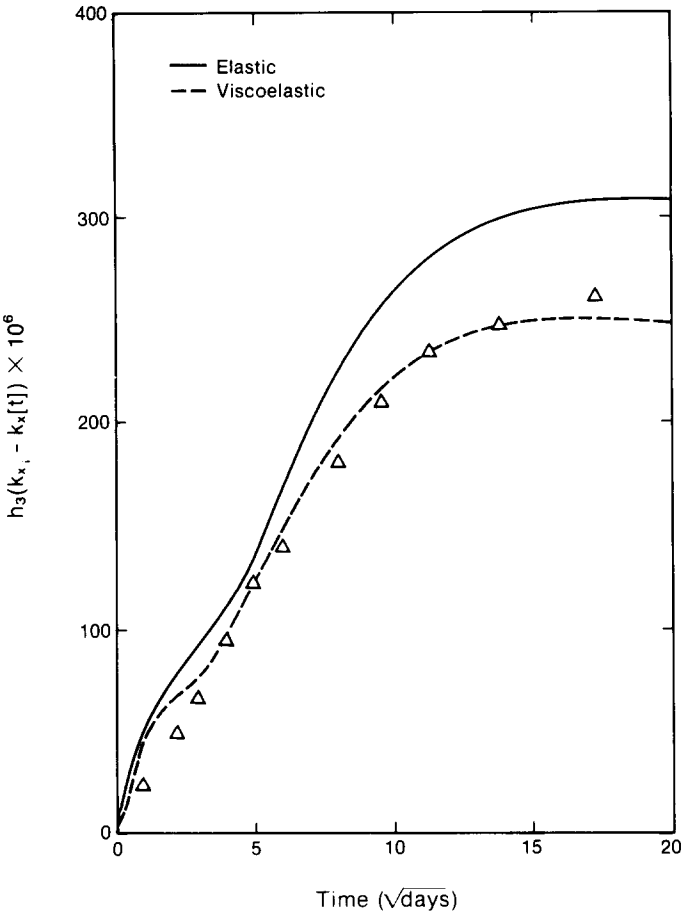

Fig. 6. Time-dependent curvature change of $(0/90/0_4/90_4/0/90)_T$ AS/3502 graphite/epoxy laminates during absorption at 327°K (130°F) 75% relative humidity.

It can be seen from Figs. 2–11 that data obtained during absorption at high temperature are closer to the elasticity predictions than to viscoelastic calculations. The data tend toward the viscoelastic results with the lowering of the conditioning temperatures. This trend indicates that, at least during initial absorption, the time-dependent behavior is predominantly viscoelastic, except under the more extreme environmental conditions. Under those more extreme conditions, the fact that measured curvatures are smaller than viscoelastic predictions suggests the presence of some sort of moisture-induced damage.

Figures 9–11 represent results obtained during absorption at a relative humidity of 13%. Because, in this case, the equilibrium moisture weight gain is 0.08%, which is below the threshold moisture content $m_1 = 0.10\%$, this circumstance is associated with no moisture-induced strains. An elastic analysis, therefore, will predict no time-dependent changes in curvature, so that only viscoelastic results are plotted in Figs. 9–11. The fact that the curvature was nevertheless observed to relax during exposure to a 13% relative humidity environment indicates that a time-dependent effect is inherently associated with moisture absorption, even in the absence of moisture-expansional strains. Note the difference in scale between Figs. 9–11 and Figs. 2–8, indicating that, under 13% R.H., the difference between experimental data and viscoelastic predictions is smaller than meets the eyes.

Periodic curvature measurements were also obtained from specimens conditioned dry at 339°K (150°F) and 327°K (130°F). The specimens were kept dry by placing a

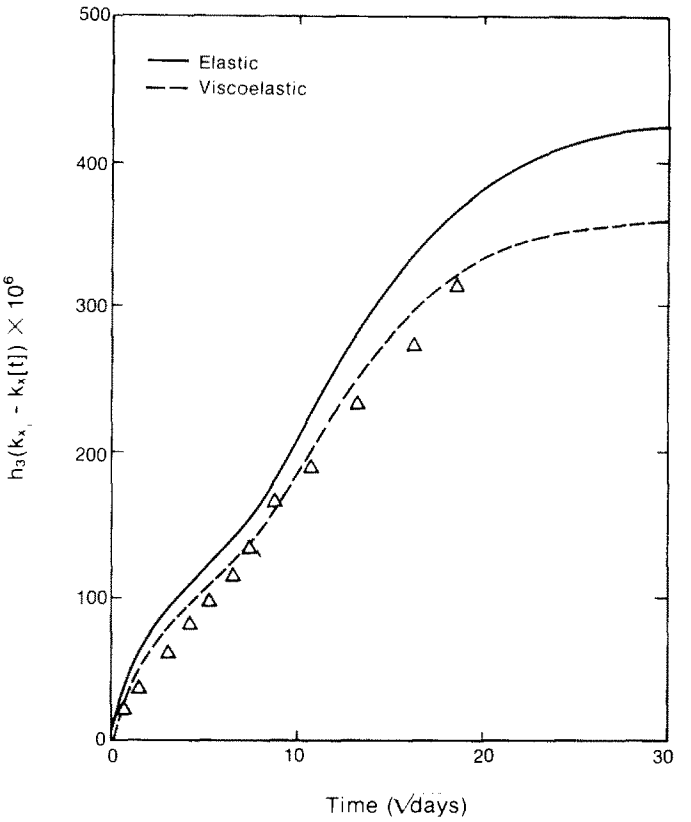

Fig. 7. Time-dependent curvature change of $(0/90/0_4/90_4/0/90)_T$ AS/3502 graphite/epoxy laminates during absorption at 298°K (77°F) 95% relative humidity.

$CaCl_2$ dessicant material in the environmental chambers. In these two situations, the measured curvature remained constant to within less than 1% of their original curvature for exposure times of approximately 6 months and 1 year, respectively. This shows that, for the AS/3502 graphite/epoxy material, time-dependent effects become significant only in the presence of moisture.

Note that, in Figs. 2–4, the measured curvatures do not return to their original values after complete desorption, indicating a hysteresis-like material response. In Fig. 2, the deviation of measured curvatures from viscoelastic predictions is about the same at the end of desorption as it is at the end of absorption. In Figs. 3 and 4, however, the deviation from the viscoelastic predictions was larger at the end of desorption than it was at the end of absorption. This is especially apparent in Fig. 4, where measured values agreed well with viscoelastic predictions at the termination of the absorption phase, but differed significantly when desorption was complete. This observation is consistent with the fact that large tensile stresses develop at the surface of the laminate during the early stages of moisture desorption due to the steep moisture gradients which occur at this time[4]. These tensile stresses enhance matrix microcracking and fiber-matrix interface degradation, thus producing smaller curvatures than would be observed in the absence of these damage mechanisms.

All the curvature data obtained under environmental conditions in which moisture expansional strains develop (e.g. Figs. 2–8) are plotted in Fig. 12. In this figure, the ordinate and abscissa have been nondimensionalized in such a way that the elastic results for all conditions fall on a single curve. The reduced time t^* is the nondimensionalized quantity $t^* = Dt/h_3^2$, m_1 is the threshold moisture content ($m_1 = 0.10\%$), while m_∞ is the equilibrium moisture content. The fact that the experimental data do not fall on a single curve provides further evidence that the material behavior is inelastic.

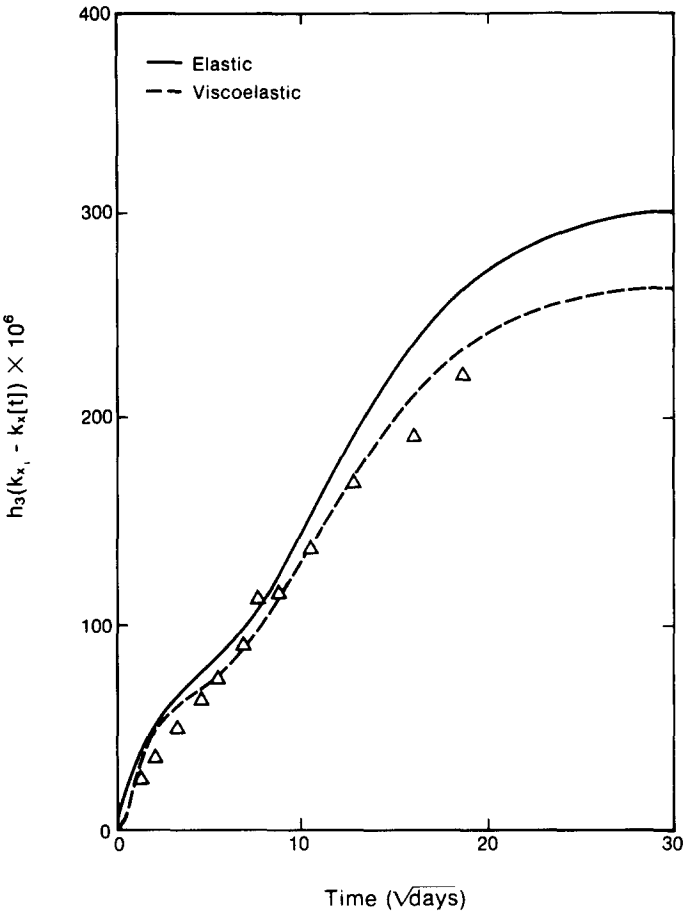

Fig. 8. Time-dependent curvature change of $(0/90/0_4/90_4/0/90)_T$ AS/3502 graphite/epoxy laminates during absorption at 298°K (77°F) 75% relative humidity.

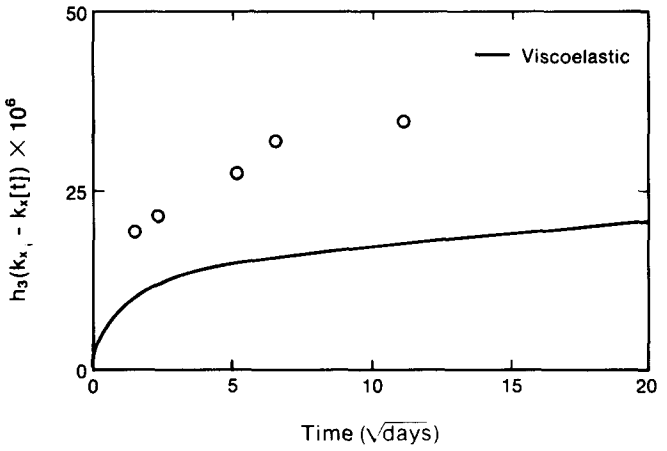

Fig. 9. Time-dependent curvature change of $(0/90/0_4/90_4/0/90)_T$ AS/3502 graphite/epoxy laminates during absorption at 339°K (150°F) 13% relative humidity.

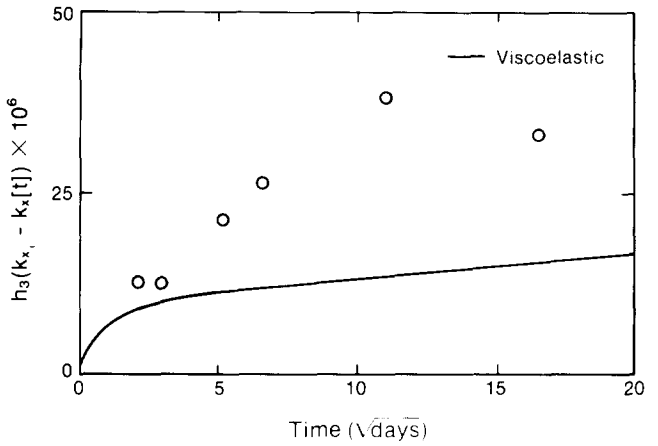

Fig. 10. Time-dependent curvature change of $(0/90/0_4/90_4/0/90)_T$ AS/3502 graphite/epoxy laminates during absorption at 327°K (130°F) 13% relative humidity.

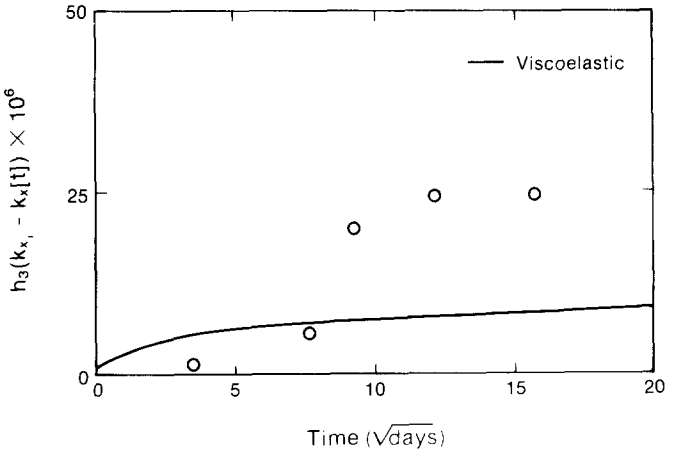

Fig. 11. Time-dependent curvature change of $(0/90/0_4/90_4/0/90)_T$ AS/3502 graphite/epoxy laminates during absorption at 298°K (77°F) 13% relative humidity.

Additional tests were performed to measure curvatures of presaturated specimens under cyclic environmental exposures. In these experiments, specimens that were saturated at 95% R.H. were switched at regular time intervals between chambers with 0% and 95% R.H. All these tests were performed at a constant temperature of 327°K (130°F).

Results for the time-dependent curvature change obtained during these tests for cycles of 16 days and 9 days are shown in Figs. 13 and 14. Note that, in these figures, time is measured from initial saturation (or the beginning of cycling). The elastic predictions are shown by solid lines, whereas viscoelastic predictions are given by dashed lines. Note that while initially the experimental results and viscoelastic predictions are in good agreement, the discrepancy between the two sets of results increases as cycling continues. This suggests that repeated wetting and drying of composites enhances the moisture-induced degradation of material properties.

This contention is further supported by the moisture uptake data obtained during the same environmental cycling tests, presented in Figs. 15 and 16. The solid lines in these figures represent predictions based upon Fick's law. Note that the discrepancies between data and theory increase as cycling proceeds. This provides an indirect confirmation to the proposition of moisture-induced damage.

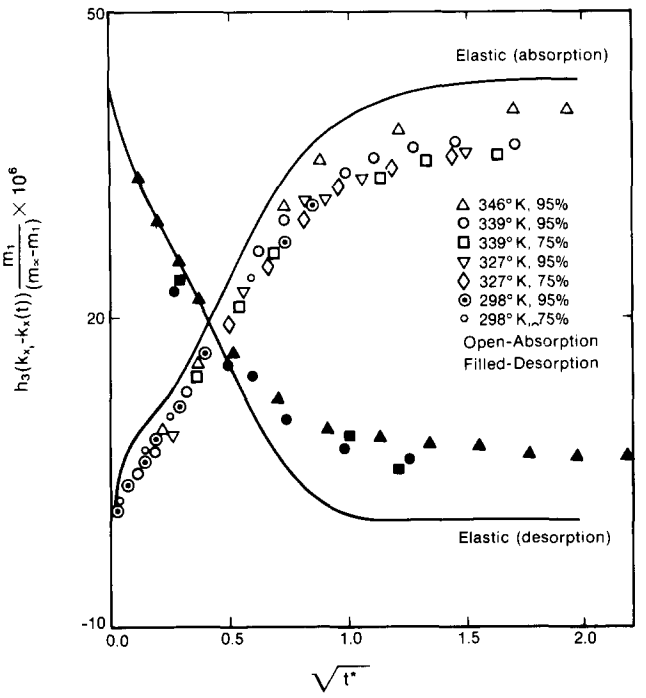

Fig. 12. Combined results for time-dependent curvature change of $(0/90/0_4/90_4/0/90)_T$ AS/3502 graphite/epoxy laminates exposed to various environmental conditions.

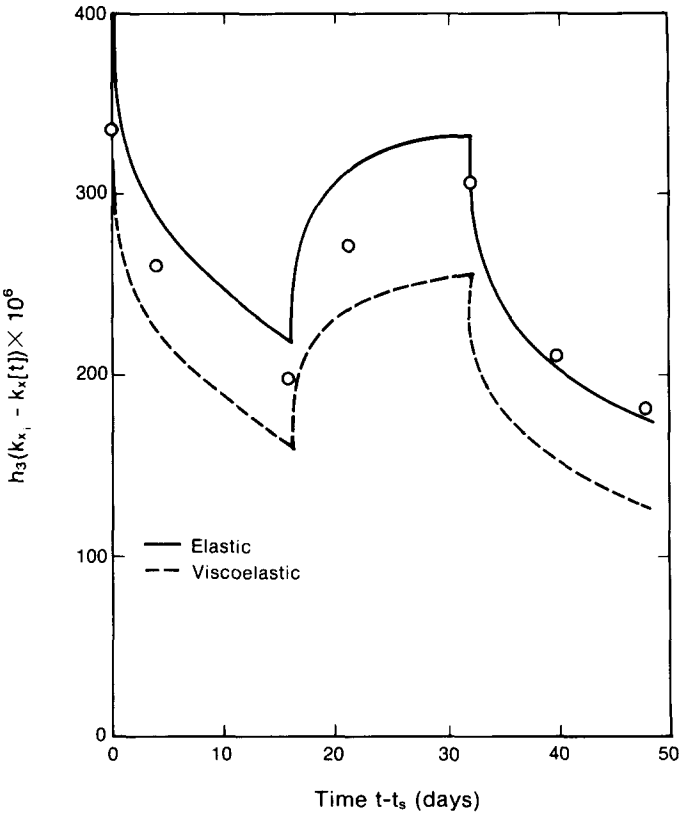

Fig. 13. Time-dependent curvature change of $(0/90/0_4/90_4/0/90)_T$ AS/3502 graphite/epoxy laminates during cyclic exposure to 0 and 95% relative humidities at 327°K (130°F), with cycle-interval of 16 days.

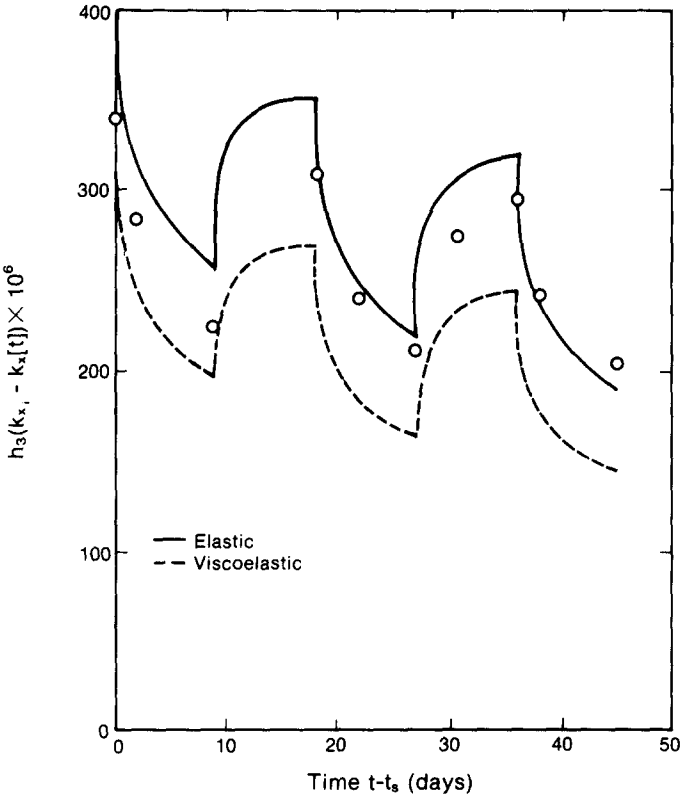

Fig. 14. Time-dependent curvature change of $(0/90/0_4/90_4/0/90)_T$ AS/3502 graphite/epoxy laminates during cyclic exposure to 0 and 95% relative humidities at 327°K (130°F) with cycle interval of 9 days.

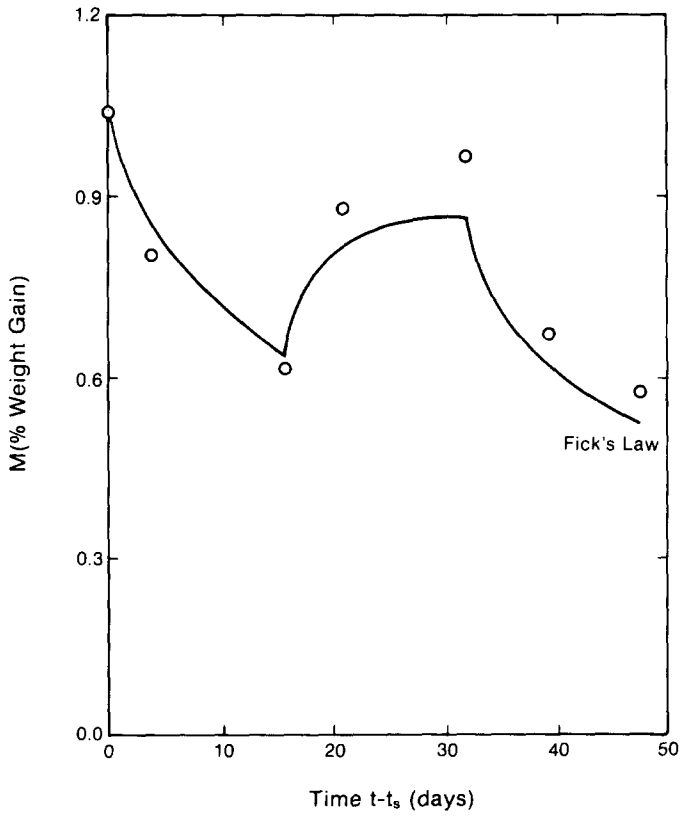

Fig. 15. Moisture content (in % weight gain) during cyclic exposure to 0 and 95% relative humidities at 327°K (130°F), with cycle interval of 16 days.

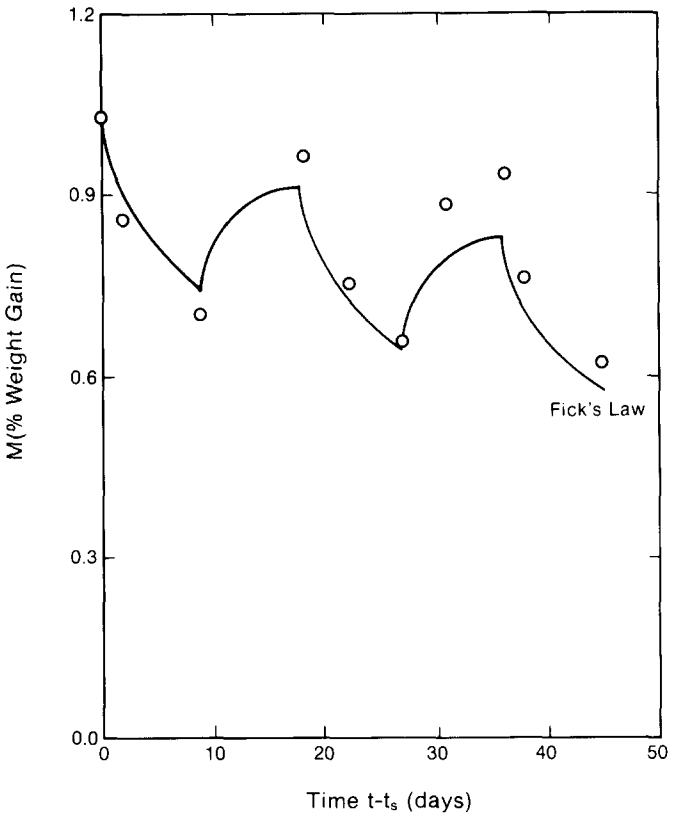

Fig. 16. Moisture content (in % weight gain) during cyclic exposure to 0 and 95% relative humidities at 327°K (130°F), with cycle interval of 9 days.

CONCLUDING REMARKS

This study presented an investigation of moisture effects on the mechanical behavior of polymeric composites. It was shown that the time-dependent material properties of the resin, which become more accentuated in the presence of moisture, play a very significant role in the response of the composite. This material time-dependence couples with the time factor associated with the diffusion process to yield a very complicated history effect.

The drying of saturated composite laminates is accompanied by tensile stresses which, under appropriate combinations of time, temperature, and humidity, exceed the tensile strength of the material—thereby causing matrix cracking or debonding between fibers and matrix. These cracks and debondings present new surfaces for moisture absorption during subsequent exposures, which lead to highly concentrated swelling strains at the newly formed tip zones. In this way, the growth of damage may feed upon itself with each additional humidity cycle until reaching a critical level.

A detailed investigation of this highly complex damage mechanism should employ fracture mechanics and deserves further study.

Acknowledgement—This work was conducted under Contract F49620-82-C-0057 from the Air Force Office of Scientific Research (AFOSR), whose support is gratefully acknowledged.

REFERENCES

1. C. C. Chamis, Residual Stresses in Angleplied Laminates and Their Effects on Laminate Behavior, NASA Report NASA TM-78835 (1978).
2. H. T. Hahn and N. J. Pagano, Curing stresses in composite laminates, *J. Comp. Mat.* **9**, 91 (1975).
3. Y. Weitsman, Effects of fluctuating moisture and temperature on the mechanical response of resin-plates, *J. Appl. Mech.* **44**, 571 (1977).

4. F. W. Crossman, R. E. Mauri and W. J. Warren, Hygrothermal damage mechanisms in graphite-epoxy composites, Lockheed Palo Alto Research Laboratory, Final Report (1979).
5. C. H. Shen and G. S. Springer, Effects of moisture on the tensile strength of composite materials, *J. Comp. Mat.* **11,** 2 (1977).
6. C. Y. Lundemo and S. Thor, Influence of environmental cycling on the mechanical properties of composite materials, *J. Comp. Mat.* **11,** 276 (1977).
7. C. E. Browning and J. T. Hartness, Effects of moisture on the properties of high performance structural resins and composites. *Proc. Third Conference on Composite Materials*, ASTM (1974).
8. R. E. Mauri, F. W. Crossman and W. J. Warren, Assessment of moisture altered dimensional stability of structural composites, *SAMPE Symp.* **23,** 1202 (1978).
9. C. E. Browning, The mechanisms of elevated temperature property losses in high performance structural epoxy resin matrix materials after exposures to high humidity environments, *Polym. Eng. Sci.* **18,** 16 (1978).
10. D. H. Kaelble, P. J. Dynes, L. W. Crane and L. Maus, Interfacial mechanisms of moisture degradation in graphite-epoxy composites, *J. Adhesion* **7,** 25 (1975).
11. K. H. G. Ashbee and R. C. Wyatt, Water damage in glass fibre/resin composites, *Proc. R. Soc.* **A312,** 553 (1969).
12. D. H. Kaelble, P. J. Dynes, L. W. Crane and L. Maus, Kinetics of environmental degradation in graphite-epoxy laminates, *Composite Reliability*, ASTM STP 580, 247 (1975).
13. M. K. Antoon and J. L. Koenig, Irreversible effects of moisture on the epoxy matrix in glass-reinforced composites, *J. Polym. Sci.: Polym. Phys.* **19,** 197 (1981).
14. I. G. Hedrick and J. B. Whitesides, Effects of environment on advanced composite structures, *Conference on Aircraft Structures: The Emerging Methodology for Structural Assurance*, AIAA, 1 (1977).
15. J. R. Vinson, R. B. Pipes, W. J. Walker and D. R. Ulrich, The effects of relative humidity and elevated temperature on composite structures, presented at the *Workshop on the Effects of Relative Humidity and Elevated Temperature on Composite Structures*, Delaware University, Newark, N.J. (1976).
16. C. D. Shirrel, Diffusion of water vapor in graphite/epoxy composites, *Advanced Composite Materials—Environmental Effects*, ASTM STP 658, 21 (1978).
17. J. M. Whitney and C. E. Browning, Some anomalies associated with moisture diffusion in epoxy matrix composite materials, *Advanced Composite Materials—Environmental Effects*, ASTM STP 658, 43 (1978).
18. O. Gillat and L. J. Broutman, Effect of an external stress on moisture diffusion and degradation in a graphite-reinforced epoxy laminate, *Advanced Composite Materials—Environmental Effects*, ASTM STP 658, 61 (1978).
19. R. DeIasi and J. B. Whiteside, Effect of moisture on epoxy resins and composites, *Advanced Composite Materials—Environmental Effects*, ASTM STP 658, 2 (1978).
20. A. Apicella, L. Nicolais, G. Astarita and E. Drioli, Hygrothermal history dependence of moisture sorption kinetics in epoxy resins, *Polym. Eng. Sci.* **21,** 18 (1981).
21. R. M. Jones, *Mechanics of Composite Materials*, Scripta Book Co. (1975).
22. C. H. Shen and G. S. Springer, Moisture absorption and desorption of composite materials, *J. Comp. Mat.* **10,** 36 (1976).
23. B. D. Harper, On the effects of post cure cool down and environmental conditioning on residual stresses in composite laminates, Ph.D. Thesis, Texas A&M University (1983).
24. A. V. Luikov, *Analytical Heat Diffusion Theory*, Academic Press, N.Y. (1968).
25. J. Crank, *The Mathematical Theory of Diffusion*, 2nd Ed. Oxford University Press, Great Britain (1975).
26. Y. Weitsman, A rapidly convergent scheme to compute moisture profiles in composite materials under fluctuating ambient conditions, *J. Comp. Mat.* **15,** 349 (1981).
27. D. A. Douglass and Y. Weitsman, Stresses due to environmental conditioning of cross-ply graphite/epoxy laminates, *Proc. Third International Conference on Composite Materials (ICCM3)*, Paris, France, 1, 529, Pergamon Press (1980).
28. R. S. Lott, Moisture and temperature effects on curvature of anti-symmetric cross-ply graphite epoxy laminates, Master's Thesis, Texas A&M University (1980).
29. R. A. Schapery, A method of viscoelastic stress analysis using elastic solutions, *J. Franklin Inst.* 279 (1965).
30. K. G. Kibler, Time-Dependent Environmental Behavior of Graphite/Epoxy Composites, *Final Report*, General Dynamics Corporation, Fort Worth, Texas, Contract No. F33615-77-C-5109, Report No. AFWAL-TR-80-4052 (1980).
31. R. A. Schapery, Viscoelastic behavior and analysis of composite materials. In *Mechanics of Composite Materials*, Vol. 2, Academic Press, N.Y. (1974).
32. F. W. Crossman, R. E. Mauri and N. T. Warren, Moisture altered viscoelastic response of graphite/epoxy composites, *Advanced Composite Materials—Environmental Effects*, ASTM STP 658, 205 (1978).
33. B. D. Harper and Y. Weitsman, Residual thermal stresses in an unsymmetrical cross-ply graphite/epoxy laminate, *Proc. 22nd SSD and Materials Conf.* Atlanta, Georgia (1981).
34. D. L. Flaggs and F. W. Crossman, Analysis of the viscoelastic response of composite laminates during hygrothermal exposure, *J. Comp. Mat.* **15,** 296 (1981).
35. M. W. Hyer, Calculations of the room-temperature shapes of unsymmetric laminates, *J. Comp. Mat.* **15,** 296 (1981).
36. F. E. M. Obrien, The control of humidity by saturated salt solutions, *J. Scient. Instrum.* **25,** 73 (1948).
37. B. D. Harper, D. Peretz and Y. Weitsman, Assessment of chemical cure-shrinkage stresses in two technical resins, *AIAA/ASME, ASCE, AHS 24th Structures, Structural Dynamics and Materials Conference* Lake Tahoe, Nevada (1983).